

Lattice QCD with eight light-quark flavors

Frank R. Brown,* Hong Chen,† Norman H. Christ, Zihua Dong,
Robert D. Mawhinney, Wendy Schaffer, and Alessandro Vaccarino†
Columbia University, Department of Physics, New York, New York 10027
(Received 29 May 1992)

QCD with eight flavors is studied on $16^3 \times N_t$ lattices with $N_t = 4, 6, 8, 16,$ and 32 , a dynamical quark mass $ma = 0.015$, and lattice coupling $\beta = 6/g^2$ between 4.5 and 5.0. For $N_t = 16$ and 32 , hadron masses and screening lengths are computed for a variety of valence quark masses. The previously observed, strong, first-order transition for $N_t = 4, 6,$ and 8 is seen, for $N_t = 16$, to become a β -independent, zero-temperature transition characterized by a factor of ≈ 3 change in lattice scale. This strong, first-order transition restores chiral symmetry, at least for $N_t = 4, 6,$ and 8 , producing a chirally symmetric, weak-coupling phase. However, as N_t increases to 16 , the chiral-symmetry properties of the weak-coupling side of the zero-temperature transition are unclear and offer a hint of a normal, finite-temperature, chiral-symmetry-breaking transition in the weak-coupling phase.

PACS number(s): 12.38.Gc, 11.15.Ha

I. INTRODUCTION

Among the possibilities offered by the numerical simulation of quantum chromodynamics (QCD) is that of studying a variety of values of the physical parameters of the system. In particular, a deeper understanding of the physics of QCD may result from studying its dependence on the dimension of the fundamental representation of the gauge group (the number of colors, N_c) and the number of quark flavors, N_f . In this paper we pursue the latter alternative by considering the case of QCD with eight light-quark flavors.

By considering a range of lattice shapes and couplings we intended to study the effects of eight quark flavors on both the finite-temperature QCD phase transition as well as the hadron spectrum at zero temperature. However, as we will see, such an investigation of the hadron spectrum is seriously impeded by the complex phase structure of eight-flavor QCD.

Our work extends earlier $T > 0$, eight-flavor calculations [1–4] to larger lattices, smaller quark masses and smaller lattice spacings, with perhaps surprising results. The earlier work on $8^3 \times 4$ [1, 3], 6^4 [2], 8^4 [2, 3] and $16^3 \times 4$ and $\times 6$ [4] lattices shows a quite strong, first-order transition. Comparing the transition for $N_f = 2, 3, 4$ and these eight-flavor calculations reveals a strengthening of the transition as the number of flavors increases [4, 5]. Both greater metastability at the critical value of β and an expanded window of small quark mass within which the transition occurs are found as N_f is increased. Regardless of the number of flavors, significant variation

of β_c is seen as the number of sites in the temperature direction, N_t , is increased from 4 to 6, as is expected for a “finite-temperature” transition.

As we show below, this pattern changes significantly for larger lattices with $N_f = 8$. First, the variation of β_c with N_t has vanished for $N_t \geq 8$; both $16^3 \times 8$ and $16^3 \times 16$ lattices show a strong, first-order transition at the same value of β . Thus the temperature-dependent transition seen for $N_t < 8$ has become a temperature-independent “bulk” transition for $N_t \geq 8$, which we describe as separating “strong”- and “weak”-coupling phases of the eight-flavor theory. (The presence of a bulk transition for large N_t is suggested by earlier N_t -independent jumps seen in $N_f = 8$ calculations with heavier quarks [2].) Second, although the valence quark mass dependence of $\langle \bar{\chi}\chi \rangle$ suggests that the transition seen for $N_t = 4, 6,$ and 8 is one of chiral-symmetry restoration (as is the case for $N_f = 2, 3,$ and 4), the situation is less clear for $N_t = 16$, where $\langle \bar{\chi}\chi \rangle$ shows nonlinear behavior for a small valence quark mass in the weak-coupling phase.

However, if β is increased to ≈ 0.3 above β_c for the bulk transition, chirally symmetric behavior is seen for both $\langle \bar{\chi}\chi \rangle$, which now depends linearly on the valence quark mass, and the hadron correlation functions. This suggests that in addition to the first-order, bulk transition separating strong- and weak-coupling phases, the weak-coupling phase may itself be divided into two distinct phases separated by a normal, finite-temperature (i.e., N_t -dependent) transition or crossover region. In fact, the nonlinear behavior seen for $\langle \bar{\chi}\chi \rangle$ in the weak-coupling phase is reminiscent of the mass dependence of $\langle \bar{\chi}\chi \rangle$ seen in four-flavor calculations on $10^3 \times 6$ when $\beta \approx \beta_c$ [6].

This behavior is described by the phase structure in the β - N_t plane shown in Fig. 1. (The figure depicts a lattice of infinite spatial extent.) The solid line represents the strong, first-order transition, which varies with N_t for $N_t < 8$ and becomes a zero-temperature or bulk transition for $N_t \geq 8$. The dashed line expresses our

*Present address: The First Boston Corporation, Park Avenue Plaza, New York, NY 10055.

†Present address: IBM Research, P.O. Box 218, Yorktown Heights, NY 10598.

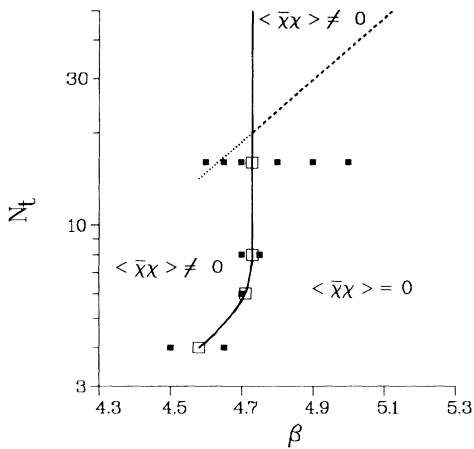


FIG. 1. A phase diagram in the β - N_t plane for eight-flavor QCD in infinite spatial volume consistent with the results presented here. N_t is the temporal extent of the lattice and $\beta = 6/g^2$ is the lattice-coupling strength. The solid line, becoming vertical for $N_t \geq 8$ locates a “zero-temperature,” first-order transition—a lattice artifact. The dashed line suggests a possible, continuum finite-temperature transition that occurs in the weak-coupling phase. The system shows chiral symmetry to the right of and below this dashed line while we speculate that chiral symmetry will be spontaneously broken to the left of and above this line. The solid squares label parameter values where we have performed simulations, while the open squares locate critical values.

speculation that a normal, finite-temperature transition or crossover region is also present in the weak-coupling phase. This line is drawn with a slope given by the perturbative renormalization group, since this gives the dependence of β_c on N_t as $N_t \rightarrow \infty$ for a physical transition and/or crossover. The N_t value of the intercept of this dashed line with the solid line is also quite uncertain and taken here to be $N_t = 20$ based on numerical evidence to be presented later.

The dotted line in Fig. 1 is an extension of the dashed line to values of β smaller than β_c for the bulk transition, since the strength of the bulk transition and the properties of our updating algorithm make it possible to study the weak-coupling phase when it is only metastable. It should be emphasized that this dotted extension of the weak-coupling, finite-temperature phase transition does not correspond to an actual phase transition line in the strong-coupling phase represented by the area to the left of the solid line. Rather it describes a metastable, “supercooled,” continuation of the weak-coupling phase into the nominal strong-coupling region. In other words Fig. 1 describes a phase diagram possessing more than one sheet, with the dotted line lying on a second sheet. The solid squares locate parameter values that we have studied and the open squares mark values of β_c that have been identified.

Unfortunately, a study of $T = 0$ hadron masses in the weak-coupling region must be performed within the wedge-shaped region in Fig. 1 that is bounded below by the dashed line and to the left by the solid line. As will

be discussed, volumes larger than 16^3 will be required to unambiguously recognize this region, let alone perform a meaningful mass calculation there.

In Sec. II we describe the calculations that have been performed and the methods used in both generating the gauge configurations studied and constructing the various observables computed. The transition for $N_f = 4, 6,$ and 8 is considered in Sec. III, where we present evidence that it separates chirally symmetric and asymmetric phases. In Sec. IV the bulk transition, isolated on $16^3 \times 16$ and $16^3 \times 32$ lattices, is discussed while in Sec. V we consider the weak-coupling phase on $16^3 \times 32$ volumes for larger β and hence higher temperature. In Sec. VI we discuss the relation between the phase structure presented here for eight flavors with that seen for smaller numbers of flavors. We suggest that the familiar cross-over region separating strong and weak coupling in the zero-flavor theory strengthens with increasing N_f and becomes our $N_f = 8$ bulk transition. Finally in Sec. VII various concluding remarks and speculations are presented.

II. DESCRIPTION OF THE CALCULATION

We have carried out a Monte Carlo evaluation of the Euclidean-space, Feynman path integral for full QCD using the R algorithm of Gottlieb *et al.* [7]. The calculation required about five months on the 256-node Columbia machine, a 16×16 mesh of fast array processors which achieves a sustained performance for these calculations of 6.4 Gflops [8]. The R algorithm evolves the gauge fields according to the action

$$\mathcal{S} = -\frac{1}{3}\beta \sum_{\mathcal{P}} \text{Re tr } U_{\mathcal{P}} - \frac{1}{4}N_f \ln \det[(D + ma)(D^\dagger + ma)]. \quad (1)$$

Here the first term is the usual Wilson action with $U_{\mathcal{P}}$ the product of the four $SU(3)$ link matrices that border the plaquette \mathcal{P} . The second term represents the effects of N_f degenerate flavors of dynamical fermions of mass m . The factor of $1/4$ preceding this term compensates for the fermion doubling present in the staggered Dirac operator D . The additional doubling introduced in Eq. (1) by squaring the Dirac operator is removed by restricting the squared operator to even lattice sites. The operator D can be defined by its action on an $SU(3)$ -triplet field ϕ :

$$(D\phi)_n = \frac{1}{2} \sum_{\mu} \eta_{n,\mu} (U_{n,\mu}^\dagger \phi_{n+\mu} - U_{n-\mu,\mu} \phi_{n-\mu}). \quad (2)$$

Here $U_{n,\mu}$ and $\eta_{n,\mu}$ are the link matrix and staggered fermion sign factor associated with a lattice link extending from the site n in the direction μ to the site $n + \mu$.

In simulating eight flavors of staggered fermions, we have a choice between two well-established methods: the R algorithm, which contains finite time-step errors of order $(\Delta\tau)^2$, and the exact hybrid Monte Carlo method of Duane, *et al.* [9], which requires twice the number of Dirac propagator inversions per unit of Monte Carlo time when used to simulate $N_f = 8$. We chose the R

algorithm with a time step $\Delta\tau = 0.0078125$ for this exploratory calculation both because code to perform the exact, eight-flavor update was not ready when we wished to begin the simulation and we wanted to reduce the required computer time. We have explicitly studied the effects of the finite time-step errors and made a comparison with results from the hybrid Monte Carlo algorithm in our determination of β_c for the transition on $16^3 \times 8$ and 16^4 lattices as is discussed in Secs. III and IV. The comparisons presented there show the expected quadratic dependence on $\Delta\tau$. Although the $\Delta\tau$ errors found are quantitatively large (e.g., 5% in β_c), the qualitative features of the calculation appear unaffected.

Thus, except where otherwise noted, this calculation is performed with a time step $\Delta\tau = 0.0078125$ and a molecular dynamics trajectory of length 0.5 time units. We have used three types of starting configurations in this calculation: hot starts where the gauge fields are disordered, cold starts where all the gauge link matrices are unit matrices and mixed starts which are described in detail in Sec. III. After each trajectory, the molecular dynamics “momenta” are randomized and measurements on the link variables carried out. In particular, after each trajectory we compute average values of the Wilson action and the fermion operator $\langle\bar{\chi}\chi\rangle$. Our gauge action is $\langle 1 - \frac{1}{3} \text{Re tr } U_{\mathcal{P}} \rangle$ and our convention for $\langle\bar{\chi}\chi\rangle$ is

$$\langle\bar{\chi}\chi\rangle \equiv \frac{1}{3} \frac{1}{N_s^3 N_t} \sum_n \langle\bar{\chi}_n \chi_n\rangle, \quad (3)$$

where the sum is over all points in the lattice. $\langle\bar{\chi}\chi\rangle$ is estimated by

$$\begin{aligned} \langle\bar{\chi}\chi\rangle &= \frac{1}{3} \frac{1}{N_s^3 N_t} \left\langle \left\langle \sum_{l,n} h_l \left(\frac{1}{D+m} \right)_{l,n} h_n \right\rangle \right\rangle \\ &= \frac{1}{3} \frac{1}{N_s^3 N_t} \left\langle \left\langle \sum_{l,n} h_l \left(\frac{m}{DD^\dagger + m^2} \right)_{l,n} h_n \right\rangle \right\rangle, \end{aligned} \quad (4)$$

where for each site n , h_n is an independent, complex three-vector of Gaussian random numbers and $\langle\langle \dots \rangle\rangle$ denotes an average over gauge fields and the random three-vectors h_n . For the work in this paper, we have used three sets of h_n 's for each gauge configuration. Also, we restrict the h_n 's to even sites in evaluating the squared operator in Eq. (4) and multiply the result by two.

Hadron propagators are calculated every 5 units of microcanonical time from quark propagators determined using Coulomb gauge wall sources whose spatial size is the spatial volume of the lattice. The quark propagator from a source at time slice t is calculated, for each color index $a = 1-3$, using as a source an SU(3)-triplet field $h_{n,t}^b$, given by

$$h_{n,t}^b = \delta_{a,b} \delta_{\bar{n}_1,0} \delta_{\bar{n}_2,0} \delta_{\bar{n}_3,0} \delta_{t',t}, \quad (5)$$

where $\bar{n} = n \bmod 2$. For a given source time slice, the three quark propagators are then combined into hadron propagators corresponding to matrix elements of the five

conventional local hadron operators [10]. In order to improve the statistical accuracy of our results, we use the average-over-time-slice (AOTS) method [11] in which this hadron propagator calculation is performed N_t times placing the wall source on each time slice in the lattice. The resulting N_t propagators are then averaged together.

In both the updating steps and the calculation of the hadron propagators we must solve a Dirac equation of the form $(D + ma)y = h$. We perform the required inversion of $D + ma$ using the conjugate gradient algorithm. We iterate this method until our approximate solution after the i th iteration y_i yields an appropriately small residual vector $r_i = [D^\dagger D + (ma)^2]y_i - (D + ma)h$. Specifically, we perform the inversion on the even sublattice (since the solution on the odd sublattice can be found from this) and iterate until

$$\sqrt{(r_i, r_i)/(h, h)} \leq \Delta, \quad (6)$$

where the inner product (a, b) of the complex vectors is over even lattice sites and colors. For the inversions that occur in the updating steps and $\langle\bar{\chi}\chi\rangle$ we use $\Delta = 6.38 \times 10^{-5}/\sqrt{N_t}$ and perform typically between 300 and 700 conjugate gradient iterations, depending on β , for $N_t = 32$. For the hadron propagator calculation we use the somewhat more stringent condition $\Delta = 2.21 \times 10^{-6}$, yielding 700 to 800 iterations for $N_t = 32$ with $ma = 0.015$.

Much is to be learned in calculations of this sort by varying the quark mass used in the simulation. Perhaps of greatest interest is the variation of $\langle\bar{\chi}\chi\rangle$ and m_π with quark mass. A nonzero value of $\langle\bar{\chi}\chi\rangle$ and a zero value m_π in the $m \rightarrow 0$ limit are both definitive indicators of the spontaneous breaking of chiral symmetry. Unfortunately, in the exploratory calculation reported here only the single value $ma = 0.015$ has been used. However, we have computed the dependence of $\langle\bar{\chi}\chi\rangle$ and the hadron masses on the quark mass that appears in the quark propagators that explicitly enter the evaluation of the right-hand side of Eq. (4) and the hadron masses. We have only considered the case where all quark propagators used to form a hadron propagator have the same quark mass.

Thus we distinguish two quark masses that enter our calculation: the “sea” quark mass m_{sea} that enters the quark determinant in the path integral and the “valence” mass m_{val} which appears in the quark propagators that make up the various observables. In this way we can define, for example, $m_\pi(m_{\text{sea}}, m_{\text{val}})$. A consistent calculation with N_f flavors of degenerate quarks requires $m_{\text{val}} = m_{\text{sea}}$. We might call the quantity $m_\pi(m_{\text{sea}}, m_{\text{val}})$ a “quenched” approximation to the proper quantity $m_\pi(m_{\text{val}}, m_{\text{val}})$. However, a non-vanishing limit of $\langle\bar{\chi}\chi\rangle$ as $m_{\text{val}} \rightarrow 0$ is nevertheless an indicator of spontaneous symmetry breakdown, although the observable in question is no longer local. Likewise the Goldstone theorem implies that if this quenched $\langle\bar{\chi}\chi\rangle(m_{\text{sea}}, m_{\text{val}})$ is non-vanishing in the limit $m_{\text{val}} \rightarrow 0$, then the corresponding $m_\pi(m_{\text{sea}}, m_{\text{val}})$ will also vanish in that limit. Clearly, the limit $m_{\text{val}} \rightarrow 0$ provides us with interesting information

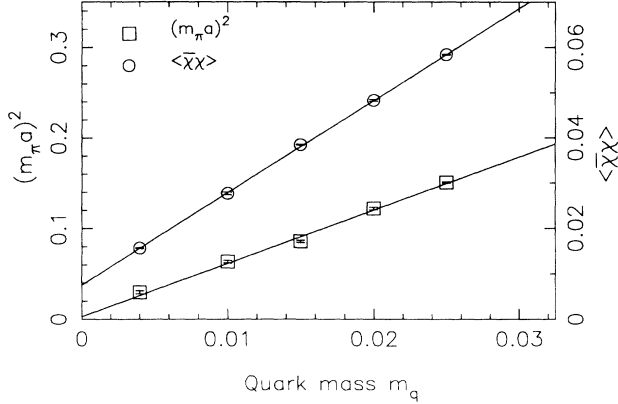


FIG. 2. The quark mass dependence seen for $\langle \bar{\chi}\chi \rangle$ and m_π^2 in earlier two-flavor calculations. The $ma = 0.01, 0.015, 0.02,$ and 0.025 points are calculations properly including the effects of dynamical quarks [12], while the $ma = 0.004$ point is obtained using that value in the explicit quark propagators but the value $ma = 0.01$ in the fermion determinant. The lines correspond to the fits in Eq. (8).

about the character of the small eigenvalues of the Dirac operator.

In fact, if the masses m_{sea} and m_{val} are sufficiently small that m_π^2 and $\langle \bar{\chi}\chi \rangle$ depend on them linearly, and if $\langle \bar{\chi}\chi \rangle$ is nonvanishing for both the limits $m_{\text{val}} = m_{\text{sea}} \rightarrow 0$ and m_{sea} fixed, $m_{\text{val}} \rightarrow 0$, then necessarily the two values of m_π^2 agree,

$$m_\pi^2(m_{\text{sea}}, m_{\text{val}}) = m_\pi^2(m_{\text{val}}, m_{\text{val}}) + O(m^2), \quad (7)$$

since both sides are linear functions of m_{val} which agree at two points, $m_{\text{val}} = m_{\text{sea}}$ and $m_{\text{val}} = 0$. Because the majority of the linear mass dependence of $\langle \bar{\chi}\chi \rangle$ comes from the quadratically divergent term proportional to m_{val} we might also expect this quenched calculation of $\langle \bar{\chi}\chi \rangle$ to be quite accurate. Our $N_f = 2$ calculations [12], in which four values of m_{sea} were used, bear these expectations out. In Fig. 2 we show m_π^2 and $\langle \bar{\chi}\chi \rangle$ for the four normal points [12] $m_{\text{val}}a = m_{\text{sea}}a = 0.01, 0.015, 0.02, 0.025$ and a fifth, quenched point [13] $m_{\text{sea}}a = 0.01, m_{\text{val}}a = 0.004$. The values for the quenched point are $m_\pi a = 0.173(5)$ and $\langle \bar{\chi}\chi \rangle = 0.0157(1)$. A linear fit to

these five points yields

$$m_\pi^2 a^2 = 0.0033(15) + 5.86(7) m_{u,d} a \quad (\chi^2/N_{\text{DF}} = 26/3), \quad (8)$$

$$\langle \bar{\chi}\chi \rangle a^3 = 0.00768(11) + 2.034(6) m_{u,d} a \quad (\chi^2/N_{\text{DF}} = 14/3).$$

Although the χ^2 for these fits is large, one can see from Fig. 2 that the $m_{\text{sea}}a = 0.015$ point is the dominant contributor to the large χ^2 , not the point at $ma = 0.004$. Leaving out the $m_{\text{sea}}a = 0.015$ point gives fits with slopes and intercepts that are the same within errors and which have $\chi^2/N_{\text{DF}} = 0.2/2$ and $0.5/2$, respectively.

III. CHIRAL-SYMMETRY RESTORATION: $N_t = 4, 6,$ AND 8

As noted in the Introduction, previous studies on lattices with $N_t \leq 8$ have observed a strengthening of the chiral transition for an increasing number of quark flavors. For $N_f = 8$, $\langle \bar{\chi}\chi \rangle$ has been seen to change by about a factor of two across the transition for quark masses of 0.1 on lattices with $N_t = 4, 6,$ and 8 [2, 4]. Previous eight-flavor work did not include an extrapolation of $\langle \bar{\chi}\chi \rangle$ to zero quark mass in the weak-coupling phase to demonstrate that the transition restored chiral symmetry. In this section we report on our investigation of this transition for $N_t = 4, 6,$ and 8 lattices—both the accurate determination of β_c and the $m_{\text{val}} \rightarrow 0$ extrapolation of $\langle \bar{\chi}\chi \rangle$ which gives evidence that this transition does restore chiral symmetry. Our $N_t = 4$ results were obtained from a series of simulations described in Table I while Tables II and III contain a similar description of the $N_t = 6$ and 8 runs. All the lattices had a spatial volume of 16^3 .

The accurate determination of β_c for a strong, first-order transition presents a familiar dilemma: if we work with a large spatial volume, the considerable metastability of both phases implies a large range of β within which each phase appears to be stable, even for quite long Monte Carlo evolution times. (At least if we use ex-

TABLE I. A list of the parameters for the runs with $N_t = 4$. The mix 1 start was produced by thermalizing a hot lattice at $\beta = 4.5$ for 80 time units and then varying β for 95 time units. The mix 2 start was produced by thermalizing a cold lattice for 70 time units at $\beta = 4.5$ and then varying β for 112.5 time units.

$\Delta\tau$	Start	β	Total τ	Valence run parameters	
				m_{val}	Valence τ
0.0078125	Mix 1	4.50	100	0.004	50–100
		4.55	25		
		4.58	100		
		4.60	15		
		4.65	200		
Mix 2		4.55	50		
		4.60	50		
		4.65	25		

TABLE II. A list of the parameters for the runs with $N_t = 6$. The mixed start was produced by thermalizing a hot lattice for 50 time units at $\beta = 4.70$ and then varying β for 135 time units.

$\Delta\tau$	Start	β	Total τ	Valence run parameters		
				m_{val}	Valence τ	
0.0078125	Mix	4.65	25	0.004	0–25	
				0.010	0–25	
		4.68	50	0.004	0–50	
				0.010	0–50	
		4.70	50	0.004	0–50	
			0.010	0–50		
			4.73	50	0.004	0–50
					0.010	0–50
	Cold	4.70	100	0.004	0–100	
					0.010	0–100
Hot	4.70	100	0.004	0–100		
			0.010	0–100		

isting, local updating algorithms.) If a sufficiently small spatial volume is used to eliminate this metastability, the transition may be significantly distorted by finite-volume effects. We solve this problem by working with a large volume but beginning with a configuration in a mixture of phases. Starting with such a mixed phase, very small changes in the choice of β cause the system to rapidly evolve into either of the two phases [14].

Our results for β_c and $\langle\bar{\chi}\chi\rangle$ at $N_t = 4, 6$, and 8 have been obtained by starting from mixed-phase configurations generated as follows: An initial β value was chosen for which hot and cold starts gave two metastable phases, with different values of $\langle\bar{\chi}\chi\rangle$ and gauge action, which were stable for 50 or more units of microcanonical time. We then chose a configuration from one phase and evolved it, changing β every 10–20 units of time until

the configuration had a value of $\langle\bar{\chi}\chi\rangle$ and action close to halfway between their values in the two phases. (Both $\langle\bar{\chi}\chi\rangle$ and the action reached their halfway values concurrently.) The final value of β used in evolving this mixed-phase configuration was chosen to keep both $\langle\bar{\chi}\chi\rangle$ and the action roughly constant for 10–20 time units, thus diminishing any “inertia” the lattice might have pushing it in the direction of either phase.

The upper curve in Fig. 3 shows the evolution of $\langle\bar{\chi}\chi\rangle$ produced when generating a mixed-phase configuration from a hot start for an $N_t = 4$ lattice. The first 80 time units show normal evolution with $\beta = 4.5$. During the next 95 time units β was continually adjusted to produce the intermediate value of $\langle\bar{\chi}\chi\rangle$ shown.

After generating a mixed-phase configuration, β_c was found by performing a series of evolutions, with different

TABLE III. A list of the parameters for the runs with $N_t = 8$. The mixed start was produced by thermalizing a cold lattice for 40 time units at $\beta = 4.60$ with $\Delta\tau = 0.0078125$ and then varying β for 60 time units. The $\Delta\tau = 0.005$ runs had a trajectory length of 0.625 time units.

$\Delta\tau$	Start	β	Total τ	Valence run parameters	
				m_{val}	Valence τ
0.0125	Mix	5.20	25	0.004	0–25
		5.25	50	0.004	0–50
		5.28	50	0.004	0–50
		5.30	50	0.004	0–50
		5.35	50	0.004	0–50
0.0078125	Mix	4.70	100	0.004	25–100
		4.73	125	0.004	75–125
		4.75	165	0.004	40–165
		4.80	50	0.004	25–50
0.005	Mix	4.60	93.75	0.004	0–93.75
		4.63	62.5	0.004	0–62.5
		4.65	62.5	0.004	0–62.5
		4.73	93.75	0.004	0–93.75
0.002	Cold	4.59	50	0.004	0–50
	Mix	4.55	105	0.004	0–105
		4.58	25	0.004	0–25
		4.60	25	0.004	0–25
		4.62	145	0.004	0–145
Exact	Mix	4.58	75	0.004	0–75
		4.60	75	0.004	0–75

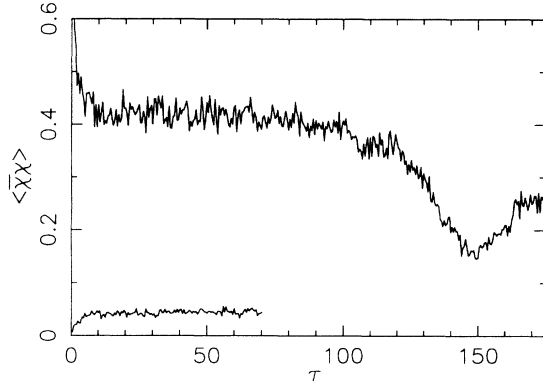


FIG. 3. Generation of a mixed-phase configuration from a hot start for $N_t = 4$. The lower, cold-start trajectory establishes the value of $\langle \bar{\chi}\chi \rangle$ for the chirally symmetric phase while the upper trajectory both gives a value of $\langle \bar{\chi}\chi \rangle$ in the symmetry-broken phase and with a subsequent tuning of β becomes our candidate “mixed” phase.

values of β , each starting from the given mixed-phase configuration. An example of this procedure is represented in Fig. 4. There we show the evolution of $\langle \bar{\chi}\chi \rangle$ for five values of β , starting from the mixed-phase configuration generated from an initial hot start. Clearly $\beta = 4.5$ lies on the strong-coupling side of the transition while $\beta = 4.65$ falls on the weak-coupling side. The slow evolution of the $\beta = 4.58$ run locates β_c while the short runs at 4.55 and 4.6 suggest $\beta_c = 4.58(1)$ as a reasonable conclusion for β_c with errors.

In order to demonstrate the reliability of this procedure we repeated the determination using a second, mixed configuration generated instead from an initial cold start. The evolutions for three choices of β shown in Fig. 5 behave in a manner very consistent with Fig. 4 and the value $\beta_c = 4.58(1)$ deduced above. This indicates that our mixed-phase configurations are independent of whether they were made from a hot or cold start and argues against any bias toward one phase. In addition, we have never seen an evolution beginning from one of our mixed-phase configurations begin to change in the direction of one phase and then reverse itself. This indi-

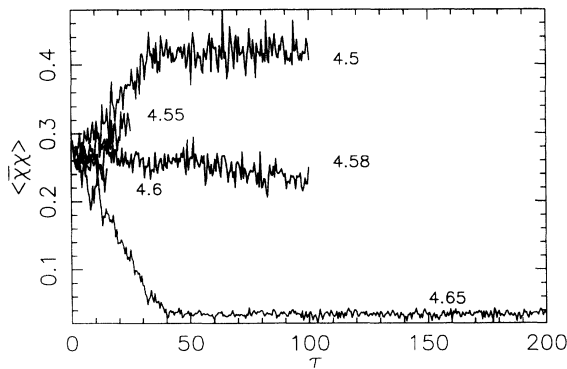


FIG. 4. Determining β_c for a mixed-phase configuration generated from a hot starting lattice with $N_t = 4$. From this figure we conclude that the critical value of β is $\beta_c = 4.58(1)$.

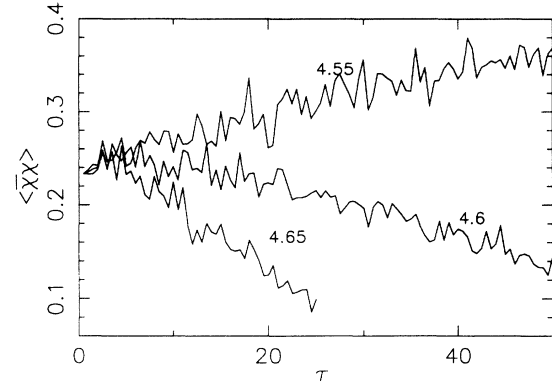


FIG. 5. Determining β_c for a mixed-phase configuration generated from a cold starting lattice with $N_t = 4$. From this figure we conclude that the critical value of β is $\beta_c = 4.58(1)$.

cates that our mixed-phase configurations have no inertia toward a particular phase.

The series of evolutions used to determine β_c for $N_t = 8$ is shown in Fig. 6, from which we deduce $\beta_c = 4.73(1)$. Although not shown, the evolutions of the action are very similar to those for $\langle \bar{\chi}\chi \rangle$. Table IV lists our results for β_c for $N_t = 4, 6,$ and 8 . For comparison this table also includes the $N_t = 16$ results which are discussed in the next section.

Given the ease with which we can determine β_c and its importance in our later considerations, it is reasonable to study the effects of finite time-step errors by computing β_c for a number of choices for $\Delta\tau$. We concentrated on the $N_t = 8$ case with the results given in Table IV. As is indicated in Table III these values of β_c were determined by the procedure described above, starting from the same mixed phase (generated with $\Delta\tau = 0.0078125$) and evolving using a series of updating schemes with $\Delta\tau = 0.002, 0.005, 0.0078125$ and 0.0125 and with the exact hybrid Monte Carlo algorithm.

Figure 7 shows the dependence of β_c on $\Delta\tau$. Leaving out the point at $\Delta\tau = 0.0125$ and the point from the exact algorithm, we find that β_c is fit by

$$\beta_c(\Delta\tau) = 4.58(1) + 2460(250) (\Delta\tau)^2 \quad (9)$$

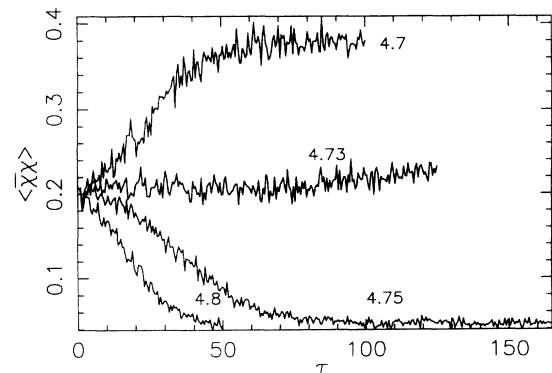


FIG. 6. Determining β_c for a mixed-phase configuration generated from a cold starting lattice with $N_t = 8$. From this figure we conclude that the critical value of β is $\beta_c = 4.73(1)$.

TABLE IV. Values for β_c for $N_t = 4, 6, 8,$ and 16 .

N_t	$\Delta\tau$	β_c
4	0.0078125	4.58(1)
6	0.0078125	4.71(1)
8	0.0125	5.29(1)
	0.0078125	4.73(1)
	0.005	4.64(1)
	0.002	4.59(1)
	exact	4.59(1)
16	0.0078125	4.73(1)
	0.005	4.62(1)

with $\chi^2/N_{\text{DF}} = 0.02/1$. (The fit for β_c using the points up to 0.0078125 is good enough to make it hard to fit the 0.0125 point, even if higher-order terms are included.) Clearly, we find the expected $(\Delta\tau)^2$ dependence of β_c and good agreement between the constant term in the fit and the value of β_c from the exact algorithm.

Finally, let us examine the values of $\langle\bar{\chi}\chi\rangle$ obtained from these various runs and their dependence on m_{val} . Tables V–VII give $\langle\bar{\chi}\chi\rangle$ for the masses used. The thermalization times τ_{eq} given in these three tables are estimates obtained by eye from the plots of $\langle\bar{\chi}\chi\rangle$ and vary because the thermalization time depends on $\beta - \beta_c$, which is not constant for the different runs.

As can be seen in Fig. 8, $\langle\bar{\chi}\chi\rangle$ extrapolates linearly to zero as $m_{\text{val}} \rightarrow 0$ for $N_t = 4, 6,$ and 8 on the $\beta > \beta_c$ side of the transition. The fits are forced through the origin and have $\chi^2/N_{\text{DF}} = 0.39/1, 3.9/2,$ and $5.1/1$, respectively. The figure clearly shows that our results are consistent with a chirally symmetric, weak-coupling phase. In addition, for $N_t = 8$ we can check that similar, chirally symmetric behavior is seen as the time step is varied by examining $\Delta\tau = 0.0125$ and 0.005 . For these cases we also find good linear fits for $\langle\bar{\chi}\chi\rangle$ as a function of quark mass. When forced through zero, the fits have $\chi^2/N_{\text{DF}} = 0.74/1$ and $0.007/1$, respectively.

IV. EVIDENCE FOR A $T=0$ TRANSITION

The eight-flavor results described in the preceding section and earlier work of others look much like the chiral-

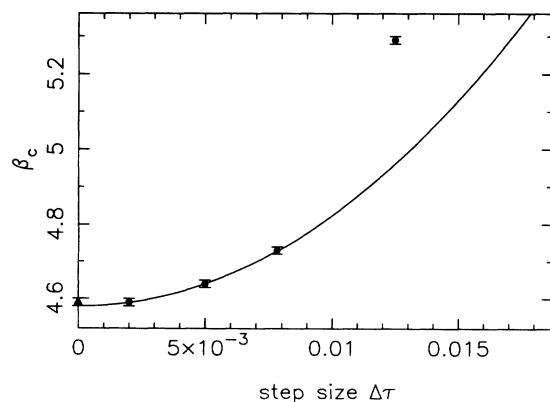


FIG. 7. β_c versus $\Delta\tau$ for $N_t = 8$. The curve is a quadratic fit to the points $\Delta\tau = 0.002, 0.005,$ and 0.0078125 .

symmetry-restoring phase transition seen for four flavors of light quarks on lattices of similar size. These results are usually interpreted as a lattice approximation to a phase transition at non-zero temperature for the continuum field theory. The variation of the value of β where the transition occurs (β_c) with N_t supports this interpretation. One expects the physical temperature of the lattice at the critical point, $T = (N_t a)^{-1}$, to be fixed so that changes in the lattice spacing a resulting from changes in β must be compensated by changes in N_t . Such behavior is quite well established in pure QCD where the variation of a (and hence N_t) with β predicted by the perturbative renormalization group is seen [15] on lattices as large as $24^3 \times 16$.

However, for the eight-flavor transition we find the critical value of β does not change when N_t is increased from 8 to 16. For $N_t = 16$ we continue to see a very strong, first-order transition even though the 16^4 lattice now has a spatial size no larger than the temporal extent. This apparent space-time volume independence of β_c suggests the transition will persist with this fixed value of β_c even for a system of infinite spatial and temporal extent. We conclude that for $N_f = 8$ there is a strong, first-order $T = 0$ or bulk transition separating the strong- ($\beta \leq \beta_c$) and weak- ($\beta \geq \beta_c$) coupling regimes.

Although the strong-coupling phase seen on 16^4 lattices appears much like that found for $N_t = 4, 6,$ and 8 , the weak-coupling phase is different in three respects. First, the precisely linear dependence of $\langle\bar{\chi}\chi\rangle$ seen in Fig. 8 for $N_t = 4, 6,$ and 8 as $m_{\text{val}} \rightarrow 0$ becomes significantly nonlinear for the 16^4 lattice. Second, for $\beta = 4.65$ $\langle\bar{\chi}\chi\rangle$ doubles as N_t is increased from 4 to 16.

Finally for $m_{\text{val}} a = m_{\text{sea}} a = 0.015$ the hadron spectrum does not show the degree of parity doubling that might be expected for a phase in which chiral symmetry has been restored. For example, we see nearly exact parity doubling for larger β as is described in Sec. V. In fact, the values of the hadron masses and $\langle\bar{\chi}\chi\rangle$ seen here at $\beta = 4.65$ are more similar to those found for two flavors in the low temperature, chirally asymmetric phase using the same quark mass and lattice size. However, we do find parity doubling in the limit $m_{\text{val}} \rightarrow 0$. We tentatively interpret these results as suggesting that these $\beta = 4.65, 16^3 \times 16$ and $\times 32$ lattices lie in a transition region that occurs in the weak-coupling phase—a finite-temperature transition and/or crossover leading to spontaneous chiral-symmetry violation on lattices of larger spatial and temporal extent.

Let us now describe these results in greater detail. Tables VIII and IX give the particulars of the $16^3 \times 16$ and $16^3 \times 32$ calculations on which our conclusions are based. Again, except where explicitly noted, we used the inexact R algorithm with the step size $\Delta\tau = 0.0078125$. Because of the limited length of some of these runs, the amount of data discarded as not in equilibrium will be discussed on a case-by-case basis below.

Figure 9 shows the evolution of $\langle\bar{\chi}\chi\rangle$ starting from hot and cold starts for $\beta = 4.65$ on a $16^3 \times 16$ lattice. The persistence of two phases over more than 300 time units, a time scale considerably greater than the initial thermalization time of ≤ 50 time units, is evidence for a strong,

TABLE V. Results for $\langle\bar{\chi}\chi\rangle$ and the gauge action for $N_t = 4$.

$\Delta\tau$	Start	β	τ_{eq}	Action	$\langle\bar{\chi}\chi\rangle$	Valence results	
						m_{val}	$\langle\bar{\chi}\chi\rangle_{\text{val}}$
0.0078125	Mix 1	4.50	50	0.6344(6)	0.418(2)	0.004	0.410(4)
		4.65	50	0.4939(1)	0.0343(3)	0.004	0.0094(4)

first-order transition. As further evidence for a first-order transition, Fig. 10 shows an evolution for the $16^3 \times 32$, $\beta = 4.60$ cold-start run in which a tunneling event occurs at $\tau \approx 250$ time units, suggesting that the weak-coupling phase becomes unstable as β is decreased from 4.65 to 4.60.

The critical coupling β_c on the 16^4 lattice is determined by the same procedure described earlier for $N_t = 4, 6$, and 8. We created a “mixed” start by beginning with the weak-coupling configuration whose evolution is shown in the lower curve in Fig. 9 and then varying β by hand for 55 time units to obtain a configuration with a value of $\langle\bar{\chi}\chi\rangle$ lying midway between the strong- and weak-coupling values seen in the figure, i.e., $\langle\bar{\chi}\chi\rangle \approx 0.2$. This final configuration is then used as the beginning for the three different runs shown in Fig. 11. This figure establishes $\beta_c = 4.73(1)$, precisely the result found above for $N_t = 8$. Because of the significant time-step dependence seen earlier for β_c , we carried out this procedure a second time for $\Delta\tau = 0.005$ and determined for that case, $\beta_c = 4.62(1)$, again in agreement with the $N_t = 8$ result for that smaller time step. We conclude that this strong, first-order transition has become independent of the lattice size for $N_t \geq 8$ and hence is a $T = 0$ transition.

The lack of dependence of β_c on N_t seen for $N_t \geq 8$ is quite consistent with the N_t dependence of the discontinuity in the gauge action across the transition. For a normal, finite-temperature transition, an increase of N_t by a factor of 2 would correspond to a decrease of the lattice spacing a by a factor of 2. Since for such a transition the discontinuity in the action is proportional to a physical latent heat, the jump in the action should decrease by a factor of $2^4 = 16$ when N_t increases from 8 to 16. In fact a similar factor of $(4/6)^4$ is seen for the $N_f = 4$ latent heat when N_t is increased from 4 to 6 [16]. However, our $16^3 \times 8$ and 16^4 results given in Tables VII and X show a large 20% jump in the action which changes relatively little between $N_t = 8$ and 16. In particular, for $N_t = 8$ the decrease in the action between $\beta = 4.70$ and 4.75 is 0.1202(5) while for $N_t = 16$ the difference between the action in the two metastable phases at $\beta = 4.65$ is 0.1150(2)—a decrease by 5% not by a factor of 16.

Next let us consider the chiral-symmetry properties of

the two phases separated by this transition. We have computed $\langle\bar{\chi}\chi\rangle$ and the hadron spectrum in each phase for a number of valence quark masses. We work at $\beta = 4.65$, where there are two metastable phases as shown in Fig. 9. Although this choice of β is below the critical value $\beta_c = 4.73$, at this β the weak-coupling phase shows no signs of instability either during the 342.5 time unit 16^4 run (Fig. 9) or the 865 time unit run on a $16^3 \times 32$ lattice. These results, together with the $\beta = 5.0$ results described in the next section are given in Tables X–XIII.

The second columns of Tables XII and XIII, for the strong-coupling phase, were obtained on a 16^4 lattice from the microcanonical time range 210–380. The fitting was done by combining these results into blocks of 5 time units and the masses came from two parameter fits assuming a single propagating state. The π mass was determined by fitting time separations 2 to 8 while the masses for the other states were obtained from time separations 1 to 5. The resulting π masses appear to be well determined from the range of time separations available. However, the correlators for the other strong-coupling states decrease so rapidly with separation that useful information comes only from a few time separations. As a result, we are less certain that those masses have taken on truly asymptotic values.

For the weak-coupling phase, given in the third column of Table XII and columns three through six of Table XIII we use the longer $\beta = 4.65$ run on a $16^3 \times 32$ lattice discarding the first 382.5 time units for equilibration. With this larger time dimension, stable results are obtained for a larger number of masses. We follow a procedure to extract the masses similar to that used earlier [12]: the π mass is obtained from a one-propagating-state, two-parameter fit while the other masses come from a two-propagating-state, four-parameter fit. We used a range of fitting separations, $t_{\text{min}} \leq t \leq 16$ as follows: For the quark masses 0.004, 0.01, and 0.015 and the N and N' states we used $t_{\text{min}} = 8$ and for all other states $t_{\text{min}} = 10$. For the quark masses 0.025 and 0.05 we used $t_{\text{min}} = 10$ for the π state and $t_{\text{min}} = 8$ for the others. With these fitting ranges we obtain $\chi^2/N_{\text{DF}} < 2$. All the masses given in Tables XII and XIII came from fits obtained by minimizing χ^2 computed from the full covariance ma-

TABLE VI. Results for $\langle\bar{\chi}\chi\rangle$ and the gauge action for $N_t = 6$.

$\Delta\tau$	Start	β	τ_{eq}	Action	$\langle\bar{\chi}\chi\rangle$	Valence results	
						m_{val}	$\langle\bar{\chi}\chi\rangle_{\text{val}}$
0.0078125	Hot	4.70	50	0.5995(4)	0.378(2)	0.004	0.371(2)
						0.010	0.375(2)
	Cold	4.70	50	0.4867(2)	0.0445(4)	0.004	0.0126(4)
						0.010	0.0302(4)

TABLE VII. Results for $\langle\bar{\chi}\chi\rangle$ and the gauge action for $N_t = 8$.

$\Delta\tau$	Start	β	τ_{eq}	Action	$\langle\bar{\chi}\chi\rangle$	Valence results	
						m_{val}	$\langle\bar{\chi}\chi\rangle_{\text{val}}$
0.0125	Mix	5.25	30	0.6908(3)	0.472(3)	0.004	0.467(5)
		5.35	30	0.4168(4)	0.0272(5)	0.004	0.0077(5)
0.0078125	Mix	4.70	70	0.6006(3)	0.378(1)	0.004	0.372(2)
		4.75	100	0.4804(4)	0.0465(3)	0.004	0.0131(3)
0.005	Mix	4.60	62.5	0.5793(5)	0.348(2)	0.004	0.341(3)
		4.73	62.5	0.4838(1)	0.0493(6)	0.004	0.0132(6)

trix. Errors were determined with the jackknife method using blocks of 15 time units (5 time units for the shorter 0.025 and 0.05 runs) with corrections for autocorrelations in Monte Carlo time.

As can be seen from Table XII the strong- and weak-coupling phases have very different values for the hadron masses. The masses in the weak-coupling phase are lighter by about a factor of 3, except the pion which we discuss in detail below. The vacuum expectation value $\langle\bar{\chi}\chi\rangle$ also becomes much smaller moving from strong to weak coupling. However, by itself, such a jump does not imply that the transition restores chiral symmetry. For example, naive scaling arguments would suggest that for small quark mass $\langle\bar{\chi}\chi\rangle$ should decrease by a factor of 3^3 when the hadron masses decrease by a factor of 3.

To study the chiral symmetry of these two phases we show the linear extrapolations of $\langle\bar{\chi}\chi\rangle$ and m_π^2 as $m_{\text{val}} \rightarrow 0$ in Figs. 12 and 13. The behavior of $\langle\bar{\chi}\chi\rangle$ and m_π^2 in the strong-coupling phase (Fig. 12) is easily interpreted. We are seeing the usual consequences of spontaneous chiral-symmetry breaking—behavior quite similar to that shown for $N_f = 2$, $\beta = 5.7$ in Fig. 2 [12, 13].

However, the chiral properties of the weak-coupling, $N_f = 8$ phase are more ambiguous. Our earlier $16^3 \times 32$ results [12, 13] for $N_f = 2$, $\beta = 5.7$ and $m_{\text{sea}}a = 0.015$ are reproduced in column five of Table XII, allowing easy comparison of the chiral-symmetry breaking found in these two sets of spectra. Although the $m_\pi - m_\sigma$ and $m_\rho - m_{A_1}$ splittings are significant for the eight-flavor case, they are perhaps half the size of those seen

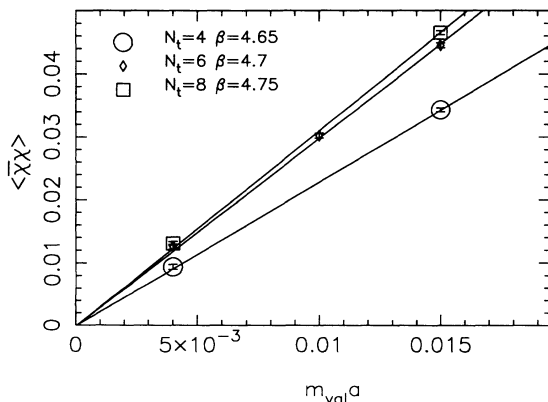


FIG. 8. Extrapolation of $\langle\bar{\chi}\chi\rangle$ for $N_t = 4, 6$, and 8 as a function of valence quark mass m_{val} . The fits are forced through the origin.

in the $N_f = 2$ case. In the earlier $N_f = 2$ calculation we found $\langle\bar{\chi}\chi\rangle = 0.0385(1)$ so the possible measure of chiral-symmetry breaking, $\langle\bar{\chi}\chi\rangle/m_\rho^3$, is the same between the two calculations up to the 20% level.

It is also of interest to ask how $\langle\bar{\chi}\chi\rangle$ changes in the weak-coupling phase as lattice size increased. We can directly compare the $N_t = 4$ and $N_t = 16$ results for $\beta = 4.65$ recognizing an increase from 0.0343(3) to 0.0711(4). Such an increase with increasing N_t might be interpreted as the onset of chiral-symmetry breaking as the temperature decreases for fixed β .

However, the notion that the weak-coupling phase seen for $N_t = 16$ and 32 shows spontaneous symmetry breaking is not supported by the dependence of $\langle\bar{\chi}\chi\rangle$ or the hadron spectrum on m_{val} . As shown in Fig. 13 $\langle\bar{\chi}\chi\rangle$ appears to approach 0 as $m_{\text{val}} \rightarrow 0$ while the corresponding limit of m_π is small but nonzero. As can be seen, the small $m_{\text{val}} \rightarrow 0$ limit of $\langle\bar{\chi}\chi\rangle$ is surprisingly nonlinear for $m_{\text{val}}a$ as small as 0.004 but certainly appears to vanish. However, the extrapolation of m_π^2 is straightforward,

$$m_\pi^2 a^2 = 0.0391(13) + 6.90(6)m_{u,d}a \quad (\chi^2/N_{\text{DF}} = 1.9/3), \quad (10)$$

giving $m_\pi^2(0) \sim 30$ standard deviations away from zero. This is in contrast with the behavior seen in the $N_f = 2$ weak-coupling phase shown in Fig. 2 where, as is shown in Eq. (8), the extrapolated π mass is consistent with zero.

In Fig. 14 we show the masses of the three parity partners $N' - N$, $A_1 - \rho$, and $\sigma - \pi$ as a function of m_{val} . Again even the considerable $\sigma - \pi$ splitting disappears linearly as $m_{\text{val}} \rightarrow 0$. Quantitatively, fitting to the three smallest values of m_{val} shown in the plot we obtain

$$\begin{aligned} m_\pi a &= 0.218(5) + 10.7(4)m_{\text{val}}a \quad (\chi^2/N_{\text{DF}} = 2.9/1), \\ m_\sigma a &= 0.220(4) + 16.5(4)m_{\text{val}}a \quad (\chi^2/N_{\text{DF}} = 5.0/1), \\ m_\rho a &= 0.359(14) + 10.8(12)m_{\text{val}}a \quad (\chi^2/N_{\text{DF}} = 0.1/1), \end{aligned} \quad (11)$$

$$\begin{aligned} m_{A_1} a &= 0.371(30) + 14.1(24)m_{\text{val}}a \quad (\chi^2/N_{\text{DF}} = 0.003/1), \\ m_N a &= 0.704(35) + 11.2(26)m_{\text{val}}a \quad (\chi^2/N_{\text{DF}} = 0.01/1), \\ m_{N'} a &= 0.694(42) + 13.5(31)m_{\text{val}}a \quad (\chi^2/N_{\text{DF}} = 0.08/1), \end{aligned}$$

showing detailed chiral-symmetry restoration as $m_{\text{val}} \rightarrow 0$. Note the linear fit to m_π^2 in Eq. (10) (using valence quark masses up to 0.050) and the linear fit to m_π in Eq. (11) (using valence quark masses up to 0.015) give 0.198(3) and 0.218(5) respectively for $m_\pi(0)$.

TABLE VIII. A list of the parameters for the runs with $N_t = 16$. The mix start was produced by thermalizing a cold lattice for 342.5 time units at $\beta = 4.65$ with $\Delta\tau = 0.0078125$ and then varying β for 55 time units.

$\Delta\tau$	Start	β	Total τ	Valence run parameters	
				m_{val}	Valence τ
0.0078125	Cold	4.65	342.5	0.004	0–215
				0.010	215–342.5
	Hot	4.65	380	0.004	0–210
				0.010	210–380
				0.010	0–40
	Mix	4.71	50		
		4.73	100	0.004	50–100
4.75		100	0.004	50–100	
0.005	Cold	4.62	350	0.004	0–350
	Hot	4.62	100	0.004	0–100
	Mix	4.60	50	0.004	0–50
		4.62	25	0.004	0–25
		4.63	25	0.004	0–25
		4.64	50	0.004	0–50

We conclude that the strong-coupling phase seen at $\beta = 4.65$ for $N_t = 16$ and 32 shows clear spontaneous violation of chiral symmetry while the chiral symmetry of the weak-coupling phase is less obvious. However, the unusual m_{val} dependence that we see in the weak-coupling phase for $\beta = 4.65$ is very much like the m_{sea} dependence found earlier in the four-flavor, $10^3 \times 6$ work of DeTar and Kogut [6]. Their results in the critical region ($\beta = 5.175$) show a nonlinear approach of $\langle \bar{\chi}\chi \rangle$ to zero as $m_{\text{sea}} \rightarrow 0$. Likewise, their π and σ screening lengths, while significantly nondegenerate for $m_{\text{sea}} = 0.05$, become equal when extrapolated linearly to $m_{\text{sea}} = 0$. This behavior is precisely the $m_{\text{val}} \rightarrow 0$ dependence that we see for these quantities. Therefore, we speculate that for $N_t = 16$ and $\beta = 4.65$, the weak-coupling phase is itself near a standard, finite-temperature transition region separating the chirally symmetric, weak-coupling behavior we see for $N_t \leq 8$ from a weak-coupling, chirally asymmetric region that will be seen for $N_t \geq 16$ on

significantly larger spatial volumes. This speculation is represented in Fig. 1, where the dashed line identifies a possible finite-temperature phase transition dividing the weak-coupling phase into low-temperature, chirally asymmetric (upper portion) and high-temperature, chirally symmetric (lower portion) phases. This line passes near $N_t = 16$ at $\beta = 4.65$ as is suggested by our results for these parameter values.

V. HIGH-TEMPERATURE REGION: $N_T = 32$

In an attempt to understand the properties of the weak-coupling phase discussed above for $\beta \approx 4.65$ on $16^3 \times 16$ and $\times 32$ lattices, let us examine a 1325 time unit calculation of $\langle \bar{\chi}\chi \rangle$ and hadron masses with $\beta = 5.0$ carried out on a $16^3 \times 32$ lattice. As is discussed below, we find clear chirally symmetric behavior for this larger value of β . The hadron screening lengths show complete

TABLE IX. A list of the parameters for the runs with $N_t = 32$. The $\beta = 4.60$ run tunneled around $\tau = 250$.

$\Delta\tau$	Start	β	Total τ	Valence run parameters	
				m_{val}	Valence τ
0.0078125	Cold	4.60	485	0.004	0–355
				0.010	355–485
	Hot	4.65	865	0.004	232.5–382.5
					532.5–765
				0.010	0–232.5
					382.5–765
				0.025	532.5–865
				0.050	765–865
				0.100	765–817.5
	0.200	817.5–865			
	Mix	4.70	100	0.004	0–100
		4.80	75	0.004	0–75
		4.90	100	0.004	0–100
		5.00	1325	0.004	1182.5–1325
				0.010	397.5–1182.5

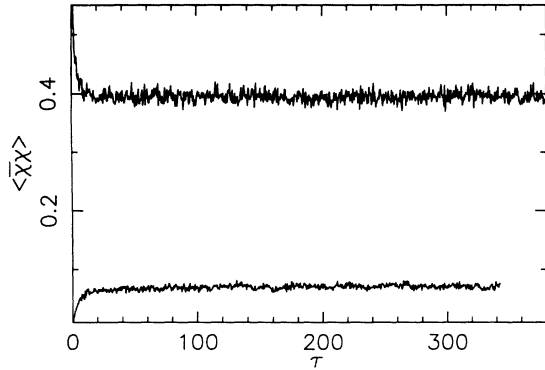


FIG. 9. The evolution of $\langle \bar{\chi}\chi \rangle$ for two independent Monte Carlo runs on a 16^4 lattice at $\beta = 4.65$. The upper curve represents a run begun with a hot start while the lower curve began with a cold start.

parity doubling within errors, $\langle \bar{\chi}\chi \rangle$ extrapolates linearly to zero as $m_{\text{val}} \rightarrow 0$ and m_π varies little as $m_{\text{val}} \rightarrow 0$ and has a relatively large $m_{\text{val}} = 0$ limit.

These masses or screening lengths were determined from the evolution interval 605–1325. The results are shown in Tables XII and XIV. The fitting procedure is very similar to that used earlier: the π -like states were determined from a two-parameter, single-state fit while the other states from a four-parameter, two-state fit. For all masses we used a fitting range from time separations 10 to 16. The quark masses of 0.01 and 0.015 were analyzed dividing the data into blocks of 15 time units while the shorter run with the valence mass of 0.004 used blocks of 5 time units. In contrast with the other mass fits discussed in this paper, the χ^2 values were very large, typically 10 to 30 with 5 degrees of freedom. However, the jackknife errors for these χ^2 values were nearly as large as the χ^2 themselves and the χ^2 computed ignoring off-diagonal terms in the correlation matrix are quite reasonable. We conclude that the fits are acceptable but that small poorly determined eigenvalues in the correlation matrix make the determination of χ^2 difficult.

The hadron spectrum looks very much like that found

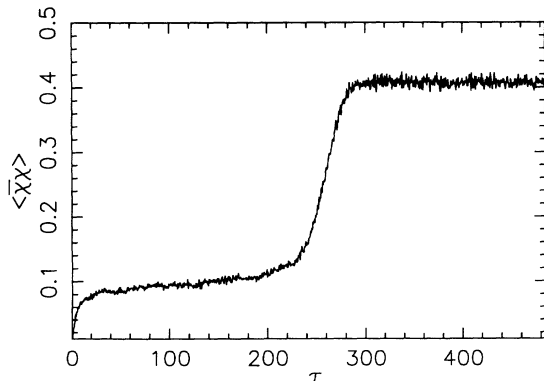


FIG. 10. The evolution of $\langle \bar{\chi}\chi \rangle$ from a cold start on a $16^3 \times 32$ lattice with $\beta = 4.60$. We interpret the jump seen at $\tau \approx 250$ as tunneling from the metastable, weak-coupling phase to the stable, strong-coupling phase.

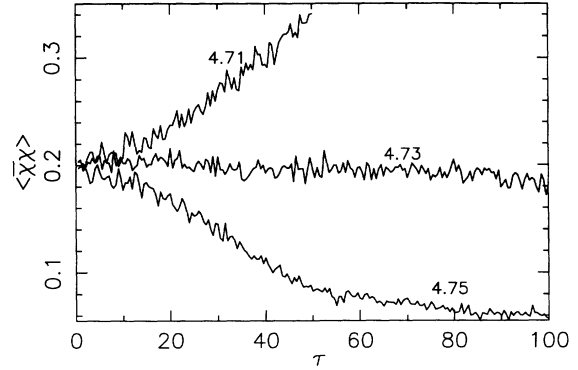


FIG. 11. Determining β_c for a mixed-phase configuration generated from a cold starting lattice with $N_t = 16$. From this figure we conclude that the critical value of β is $\beta_c = 4.73(1)$.

in earlier calculations in the plasma phase [6]. In particular the masses (or more accurately screening lengths) show remarkable parity doubling with the parity partners $\pi - \sigma$, $\rho - A_1$, and $N - N'$ having very nearly the same mass. Likewise we can examine the extrapolation to zero valence mass of both m_π^2 and $\langle \bar{\chi}\chi \rangle$ shown in Fig. 15. Linear fits to the data yield

$$m_\pi^2 a^2 = 0.134(6) + 1.95(52) m_{\text{val}} a \quad (\chi^2/N_{\text{DF}} = 2.0/1),$$

$$(12)$$

$$\langle \bar{\chi}\chi \rangle a^3 = 0.00052(9) + 2.326(7) m_{\text{val}} a \quad (\chi^2/N_{\text{DF}} = 8.2/1).$$

In marked contrast with the behavior seen for $\beta = 4.65$, m_π depends rather weakly on the valence quark mass, extrapolating to a value only 10% below the $m_{\text{val}} = 0.015$ point, while $\langle \bar{\chi}\chi \rangle$ extrapolates to a very small value. Given the nonvanishing of m_π^2 as $m_{\text{val}} \rightarrow 0$, the statistically nonzero value of $\langle \bar{\chi}\chi \rangle$ may reflect the use in Eq. (12) of a fit neglecting the correlations between results for different valence quark masses.

Although the behavior seen for $\beta = 5.0$ is very clearly that expected from QCD at finite temperature, we should emphasize that our $16^3 \times 32$ lattice is awkward to interpret as representing finite temperature. The nominal “temperature” direction with extent $N_t = 32$ and the required antiperiodic boundary conditions for the fermions is the longest dimension in the lattice. Probably the best interpretation of our space-time volume is as a $16^2 \times 32$ spatial volume with a temperature dimension corresponding to 16 lattice units. Clearly the behavior seen on this $16^3 \times 32$ lattice may show significant finite-volume distortions relative to a proper, finite-temperature calculation on a $N_s^3 \times 16$ lattice with $N_s \gg 16$.

The contrast between the $\beta = 5.0$ behavior just described and the $\beta = 4.65$, weak-coupling phase discussed

TABLE X. Results for $\langle\bar{\chi}\chi\rangle$ and the action for $N_t = 16$.

$\Delta\tau$	Start	β	τ_{eq}	Action	$\langle\bar{\chi}\chi\rangle$	Valence results	
						m_{val}	$\langle\bar{\chi}\chi\rangle_{\text{val}}$
0.0078125	Cold	4.65	100	0.4961(1)	0.0711(4)	0.004	0.0259(5)
						0.010	0.0541(5)
0.005	Hot	4.65	100	0.6111(2)	0.3953(4)	0.004	0.3900(11)
						0.010	0.3933(6)
0.005	Cold	4.62	100	0.5006(1)	0.0829(6)	0.004	0.0399(8)
						0.004	0.305(2)
	Hot	4.62	75	0.5631(3)	0.314(1)		

in Sec. IV supports the hypothesis that for the 16^4 lattice, $\beta = 4.65$ lies near a transition region. By increasing β from 4.65 to 5.0 the degree of chiral symmetry has dramatically increased for fixed $m_{\text{val}} = 0.015$ and the nonlinear m_{val} dependence of $\langle\bar{\chi}\chi\rangle$ has disappeared.

VI. POSSIBLE N_f -DEPENDENCE OF QCD

In this section we present a possible picture of the N_f dependence of QCD that connects earlier work for $N_f = 0, 2, 3,$ and 4 with the $N_f = 8$ results given here. Although the picture described below is supported by the presently available numerical results, it is far from unambiguously established by our current calculations.

We would like to interpret the eight-flavor bulk transition seen here as an outgrowth of the strong- to weak-coupling crossover region seen in pure SU(3) gauge theory for $\beta \approx 5.6$. The variation seen in this region provides a connection between strong coupling, where the scale of the physics is controlled by the lattice spacing, and weak coupling, where the scale is unrelated to the lattice spacing. (The width of the crossover region for SU(2) seen using the standard Wilson action can be altered by including an adjoint representation contribution to the action [17].) As one passes through this region from strong to weak coupling, the hadronic energy scale (measured in lattice units) decreases at a rate faster than predicted by the perturbative renormalization group. This was seen quite clearly for $T_c a$ in pure SU(3) by Kennedy *et al.* [18].

We hypothesize that adding additional light dynamical quarks to QCD promotes a rapid crossover region

to a phase transition, the first-order, bulk transition seen here, and that the addition of the quarks is similar to the effect of a nonzero adjoint action in the pure SU(2) case. The effect of this increasingly sharp crossover region on the finite-temperature QCD phase transition might be deduced from Fig. 16. Here we represent the crossover region for a system of infinite space-time volume by the interval of β between the vertical dotted lines. The more rapid variation of N_t with β_c within this region joins the relatively large value of $T_c a$ for small β with a smaller value for large β . If this region narrows as the number of flavors increases, sharpening into an actual discontinuity, the QCD phase transition for values of β_c within this crossover region might be expected to sharpen as well. Such a sharpening of the transition as the number of flavors increases is certainly well established by current simulations [5].

Furthermore, such a narrowing of the crossover region with increasing N_f would imply a corresponding increase in slope of N_t versus β within this region. In Fig. 17 we plot the variation of N_t with β_c seen in simulations for zero [19], two [20], and four [21] flavors together with that seen here for $N_f = 8$. For the two and four flavor cases, linear interpolation has been used to produce a value for β_c at $m_{\text{sea}} a = 0.015$. The behavior predicted by the perturbative renormalization group is shown by the slopes of the dashed lines in the figure. This figure is consistent with the view that temperature dimensions between $N_t = 4$ and 8 lie within this crossover region and that the slope of the N_t -versus- β_c curve is increasing with N_f .

Although far from well established, this picture is nicely consistent with the eight-flavor results presented

TABLE XI. Results for $\langle\bar{\chi}\chi\rangle$ and the action for $N_t = 32$. The $\beta = 4.60$ run tunneled at about $\tau = 250$.

$\Delta\tau$	Start	β	τ_{eq}	Action	$\langle\bar{\chi}\chi\rangle$	Valence results	
						m_{val}	$\langle\bar{\chi}\chi\rangle_{\text{val}}$
0.0078125	Cold	4.60	325	0.62031(6)	0.4075(3)	0.004	0.4038(16)
						0.010	0.4053(4)
		4.65	382.5	0.49552(6)	0.0687(1)	0.004	0.0234(3)
						0.010	0.0506(3)
						0.025	0.0983(1)
						0.050	0.1532(2)
						0.100	0.2255(2)
						0.200	0.3390(2)
		5.00	250	0.45125(2)	0.03539(3)	0.004	0.00965(9)
						0.010	0.02386(4)

TABLE XII. Hadron masses for quark mass $m_{\text{val}}a = m_{\text{sea}}a = 0.015$. The second column was obtained on a 16^4 lattice beginning with a hot start and the third and fourth on $16^3 \times 32$ lattices with a cold start. For reference, the right column lists the results of our earlier $N_f = 2$, $16^3 \times 32$ calculation with $m_{\text{sea}}a = m_{\text{val}}a = 0.015$ [11–13].

(J^{PC})	$\beta = 4.65$ strong	$\beta = 4.65$ weak	$\beta = 5.00$	$\beta = 5.7$
$\pi(0^{-+})$	0.297(1)	0.378(2)	0.405(3)	0.293(2)
$\pi_2(0^{-+})$	1.60(8)	0.471(7)	0.434(10)	0.333(3)
$\sigma(0^{++})$		0.465(3)	0.415(4)	0.487(12)
$\rho(1^{--})$	1.41(1)	0.522(7)	0.484(7)	0.455(8)
$\rho_2(1^{--})$	1.64(2)	0.521(4)	0.490(5)	0.452(7)
$A_1(1^{+-})$		0.582(11)	0.491(7)	0.594(22)
$N(\frac{1}{2}^+)$	2.29(7)	0.872(10)	0.807(7)	0.685(10)
$N'(\frac{1}{2}^-)$		0.896(13)	0.810(6)	0.833(38)
$B_1(1^{++})$		0.586(26)	0.512(8)	0.596(28)

in this paper. If the crossover region shown in Fig. 16 shrinks to a vertical line as $N_f \rightarrow 8$, the finite-temperature phase transition effectively disappears for the corresponding interval of N_t , being engulfed there by the bulk transition. An eight-flavor phase diagram very much like that shown in Fig. 1 results, in a manner that might be described as follows.

(1) For strong coupling and small values of N_t one expects to see a single phase transition that separates very different strong- and weak-coupling regimes. N_t should vary with β for small values of N_t characteristic of the small length scale important at strong-coupling ($4 \leq N_t \leq 8$ in Fig. 1).

(2) For values of N_t larger than this strong-coupling length scale, the transition becomes a bulk transition, with a fixed value of $\beta = \beta_c$. Now the dramatic change in hadronic length scale, which occurred rapidly in the crossover region for $N_f \leq 4$, happens discontinuously across this bulk transition (a scale change by a factor of 3 in our case for $N_t \geq 8$). The finite-temperature,

N_t -dependent transition has disappeared.

(3) An apparently independent finite-temperature transition should occur in the weak-coupling phase at a much larger value of N_t . This larger value of N_t (determined for β near the bulk transition) should be related to the values of N_t identified in 1 above. These two scales should be related by the same factor that describes the jump in the length scale of hadronic phenomena across the bulk transition. Thus, in our case we might expect a weak-coupling, finite-temperature phase transition to occur for $\beta = 4.73$ and values of N_t in the range of 3 (the jump in hadronic length scale) $\times 8$ (the N_t where the transition becomes N_t independent). In fact, as discussed in Sec. IV, we have some evidence for such a weak-coupling, finite-temperature transition for $\beta = 4.65$ and $N_t \approx 16$. A choice of $\beta = 4.73$ and $N_t = 20$ is used to locate the dashed curve in Fig. 1.

We can compare the ratio T_c/m_ρ for this conjectured finite-temperature transition with the value for other numbers of flavors. For zero, two, and four flavors, ex-

TABLE XIII. Hadron masses calculated with a variety of valence quark masses. The masses quoted in the second column were obtained on a 16^4 lattice beginning with a hot start while those in columns three through six came from a cold start using a $16^3 \times 32$ lattice.

(J^{PC})	$\beta = 4.65$ strong		$\beta = 4.65$ weak		
	$m_{\text{val}}a = 0.01$	$= 0.004$	$= 0.01$	$= 0.025$	$= 0.05$
$\pi(0^{-+})$	0.243(1)	0.257(4)	0.328(2)	0.465(4)	0.619(2)
$\pi_2(0^{-+})$	1.65(12)	0.369(32)	0.420(6)	0.564(5)	0.767(7)
$\sigma(0^{++})$		0.284(3)	0.391(3)	0.587(5)	0.790(6)
$\rho(1^{--})$	1.40(2)	0.404(11)	0.465(9)	0.632(6)	0.813(4)
$\rho_2(1^{--})$	1.63(2)	0.407(11)	0.468(7)	0.634(7)	0.817(7)
$A_1(1^{+-})$		0.428(28)	0.511(14)	0.751(40)	0.951(26)
$N(\frac{1}{2}^+)$	2.40(15)	0.747(30)	0.818(21)	0.992(15)	1.246(8)
$N'(\frac{1}{2}^-)$		0.744(34)	0.836(28)	1.043(31)	1.304(29)
$B_1(1^{++})$		0.429(21)	0.511(24)	0.765(45)	1.045(73)

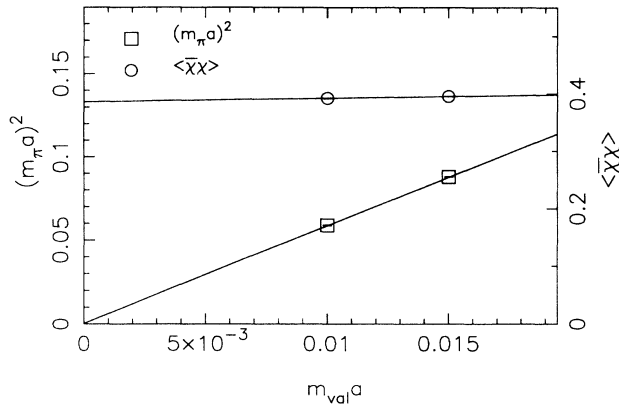


FIG. 12. Linear fits to $\langle \bar{\chi}\chi \rangle$ and m_π^2 in the strong-coupling phase at $\beta = 4.65$ on a 16^4 lattice. The m_π^2 fit is forced through the origin and has $\chi^2/N_{\text{DF}} = 0.1/1$.

trapolated to zero quark mass, $T_c/m_\rho = 0.26, 0.19$ and 0.13 [5]. Using m_ρ at $\beta = 4.65$ and assuming a monotonic decrease in T_c/m_ρ with the number of flavors, we find $N_t \geq 21$.

Of course, a $T = 0$ or bulk transition for which β_c becomes precisely independent of N_t should separate two phases each of whose properties are independent of N_t . This is not the case for a quark-gluon plasma, a natural candidate for the high temperature, weak-coupling phase represented by the lower right region of Fig. 1. However, the $1/N_t^4$ behavior expected for the free energy of a quark-gluon plasma becomes sufficiently weak for $N_t \geq 8$ as to be completely consistent with the N_t dependence of β_c that we see. In fact, $\beta_c(N_t)$ for our four values of N_t is well fit by

$$\beta_c(N_t) = 4.737(6) - 40(3)/N_t^4, \quad \chi^2/N_{\text{DF}} = 0.6/2. \quad (13)$$

A final implication of our hypothesis, in analogy with the pure SU(2) case, is that for large N_t , the strong- and weak-coupling sides of the bulk transition may be contin-

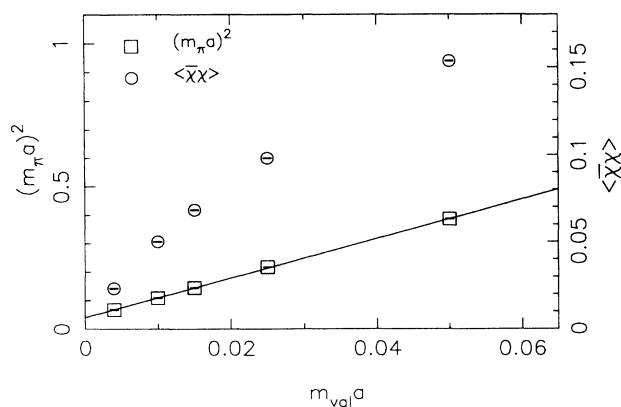


FIG. 13. $\langle \bar{\chi}\chi \rangle$ and m_π^2 in the weak-coupling phase at $\beta = 4.65$ on a $16^3 \times 32$ lattice. The line is a linear fit to m_π^2 .

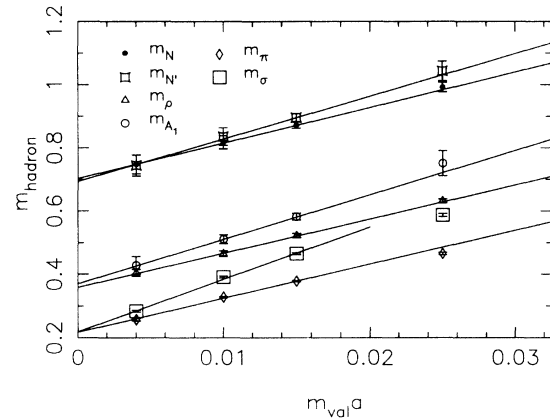


FIG. 14. Values $m_\pi, m_\sigma, m_\rho, m_{A_1}, m_N$, and $m_{N'}$ plotted versus $m_{\text{val}} a$ for a $16^3 \times 32$ lattice in the weak-coupling phase with $\beta = 4.65$. The lines shown correspond to the fits in Eq. (11).

uously connected by using an action which includes single plaquette contributions from higher representations of SU(3). This is consistent with our picture that the bulk transition, for large enough lattices, is between two chirally asymmetric phases.

VII. CONCLUSION

Our $N_f = 8$ studies are well summarized by the $\beta - N_t$ phase diagram given in Fig. 1. Let us conclude with the following remarks.

(1) We have argued in Sec. VI that the phase structure shown in Fig. 1 may be quite consistent with the flavor dependence of the QCD phase transition seen previously for $N_f = 0, 2, 3$, and 4. However, in that discussion we argued that the well-known strengthening of the finite-temperature transition for $4 \leq N_t \leq 8$ that is seen with increasing N_f came from approaching the strong, $N_f = 8$ bulk transition. Thus this important feature, which dom-

TABLE XIV. Hadron masses for two different valence quark masses on a $16^3 \times 32$ lattice.

(J^{PC})	$\beta = 5.00$	
	$m_{\text{val}} a = 0.004$	$m_{\text{val}} a = 0.01$
$\pi(0^-)$	0.386(9)	0.389(3)
$\pi_2(0^-)$	0.500(108)	0.422(27)
$\sigma(0^{++})$	0.384(9)	0.394(5)
$\rho(1^{--})$	0.474(6)	0.465(10)
$\rho_2(1^{--})$	0.485(8)	0.481(8)
$A_1(1^{+-})$	0.475(6)	0.469(10)
$N(\frac{1}{2}^+)$	0.783(22)	0.785(8)
$N'(\frac{1}{2}^-)$	0.789(28)	0.786(7)
$B_1(1^{++})$	0.487(8)	0.491(11)

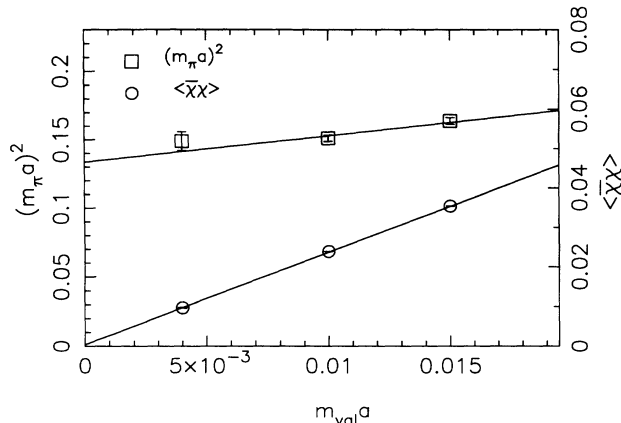


FIG. 15. $\langle \bar{\chi}\chi \rangle$ and m_{π}^2 plotted as a function of $m_{\text{val}}a$ for $\beta = 5.00$ on a $16^3 \times 32$ lattice. The straight lines shown are least squares fits to the three mass values $m_{\text{val}}a = 0.004, 0.01,$ and 0.015 . Both quantities show the behavior expected in a chirally symmetric phase.

inates present lattice calculations, may be closely tied to a lattice artifact. The true, continuum, N_f dependence of the QCD phase transition may be quite different and may be seen only on much finer lattices.

(2) It is interesting to ask if such a bulk transition for eight flavors may have already been anticipated. In fact there have been a number of papers that have explored possible phase structures for QCD with a large number of quark flavors [23, 2]. Surely interesting new behavior is to be expected as one approaches $N_f = 16.5$ where asymptotic freedom is lost. However, these theoretical studies typically predict a transition between a strong-coupling, chirally asymmetric phase with particle-like bound states and a zero-temperature, weak-coupling

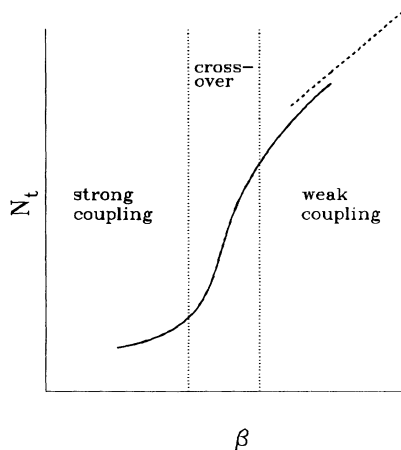


FIG. 16. A sketch of the β_c dependence of N_t for the finite-temperature QCD phase transition for $N_f \leq 4$. The area between the vertical, dotted lines represents the region of β for which infinite space-time volume systems show cross-over behavior from strong to weak coupling. The increased slope of the N_t -versus- β_c curve in this region displays the well-established non-scaling behavior seen for $T_c a$ in this region. The dashed line has a slope predicted by the perturbative renormalization group.

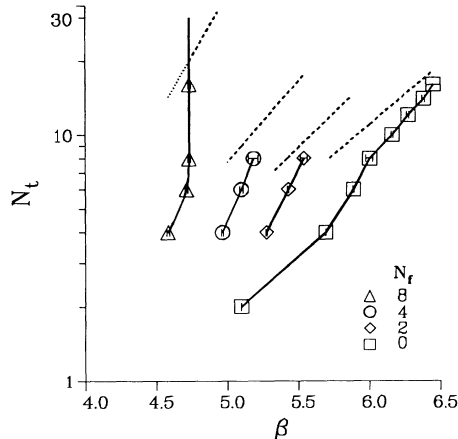


FIG. 17. Values of N_t versus β_c are plotted for zero [19], two [20], four [21] and eight flavors. The dashed lines have slopes predicted by the perturbative renormalization group and have been located to show the possible weak-coupling behavior of the adjacent curve.

phase with Green's functions showing fractional anomalous dimension and lacking a particle interpretation.

This behavior is not seen in the weak-coupling phase of Fig. 1 for either $\beta = 4.65$ or 5.0 . The masses or screening lengths given in Tables XII–XIV are nonzero and come from fitting the correlation function to a function with exponential time dependence. Thus it is most natural to interpret these mass results as describing interacting, particlelike states with definite, nonzero-energy eigenvalues. We believe that the high-temperature, weak-coupling phase seen in our calculations is quite conventional, very much like normal, high-temperature QCD seen for $N_f \leq 4$.

(3) A further argument for the finite-temperature transition represented by the dashed line in Fig. 1 is based on the 't Hooft anomaly conditions [22]. Since the 't Hooft anomaly conditions are inconsistent with a chirally symmetric eight-flavor, color SU(3) theory at zero temperature, we expect that the chirally symmetric phase to the right of the bulk transition in Fig. 1 cannot extend to zero temperature in the continuum limit. The finite-temperature transition suggested by the dashed line in Fig. 1 ensures that this chirally symmetric phase is restricted to a region of nonzero temperature in the continuum, $N_t \rightarrow \infty$ limit.

(4) Our original objective in undertaking these eight-flavor calculations was to study the zero-temperature hadron spectrum for $N_f = 8$ to gain some quantitative insight into the effects of the fermion determinant in lattice QCD, hadron mass calculations. This objective has been frustrated by the existence of the $N_f = 8$ bulk transition.

The decrease in T_c/m_{ρ} expected as N_f increases, requires that we increase $m_{\rho} a$ by lowering β or increase $1/Ta = N_t$ relative to calculations with smaller N_f . The $N_f = 8$ bulk transition prevents us from increasing $m_{\rho} a$ by moving closer to the strong-coupling region and forces us to work instead at larger N_t , in particular lattice sizes with spatial dimensions $\geq N_t \gg 16$. Thus it

appears that both a proper demonstration of the finite-temperature, weak-coupling phase transition and such a low-temperature study of hadron masses in eight-flavor QCD forces the use of lattice volumes considerably larger than $16^3 \times 32$.

After the completion of this work, we became aware of a study of QCD with many flavors of Wilson fermions in the strong coupling limit ($\beta = 0.0$) [24]. Given the difference in the coupling and the type of fermions used, the overlap between [24] and the present work is unclear.

ACKNOWLEDGMENTS

Helpful conversations with S. Chandrasekharan, A. Gocksch, S. Gottlieb, F. Karsch, G. Kilcup, W. Lee, A. Mueller, B. Svetitsky, D. Toussaint, and D. Zhu are gratefully acknowledged. We are especially indebted to S. Kim, D. Sinclair, and their colleagues at Argonne whose discussions originally attracted our interest to this subject. This research was supported in part by the U.S. Department of Energy.

-
- [1] J. B. Kogut, J. Polonyi, H. W. Wyld, and D. K. Sinclair, *Phys. Rev. Lett.* **54**, 1475 (1985).
- [2] J. B. Kogut and D. K. Sinclair, *Nucl. Phys.* **B295** [FS21], 465 (1988).
- [3] M. Fukugita, S. Ohta, and A. Ukawa, *Phys. Rev. Lett.* **60**, 178 (1988).
- [4] S. Ohta and S. Kim, *Phys. Rev.* **44**, 504 (1991); Columbia University report (in preparation).
- [5] For a recent review of finite-temperature QCD with $N_f = 2, 3$, and 4, see S. Gottlieb, in *Lattice '90*, Proceedings of the International Symposium, Tallahassee, Florida, 1990, edited by U. M. Heller, A. D. Kennedy, and S. Sanieievici [*Nucl. Phys. B (Proc. Suppl.)* **20**, 247 (1991)].
- [6] C. DeTar and J. B. Kogut, *Phys. Rev. Lett.* **59**, 399 (1987); *Phys. Rev. D* **36**, 2828 (1987).
- [7] S. Gottlieb *et al.*, *Phys. Rev. D* **35**, 2531 (1987).
- [8] A. Vaccarino, in *Lattice '89*, Proceedings of the International Symposium, Capri, Italy, 1989, edited by R. Petronzio *et al.* [*Nucl. Phys. B (Proc. Suppl.)* **17**, 421 (1990)]; N. H. Christ, *ibid.* p. 267.
- [9] S. Duane *et al.*, *Phys. Lett. B* **195**, 216 (1987).
- [10] K. C. Bowler, *Nucl. Phys.* **B284**, 299 (1987).
- [11] H. Chen, in *Lattice '90* [5], p. 370.
- [12] F. R. Brown *et al.*, *Phys. Rev. Lett.* **67**, 1062 (1991).
- [13] H. Chen, Ph.D. thesis, Columbia University, 1991; F. R. Brown *et al.* (in preparation).
- [14] For an early application of this technique, see M. Creutz, L. Jacobs, and C. Rebbi, *Phys. Rev. Lett.* **42**, 1390 (1979).
- [15] S. A. Gottlieb *et al.*, *Phys. Rev. Lett.* **55**, 1958 (1985); N. H. Christ and A. E. Terrano, *Phys. Rev. Lett.* **56**, 111 (1986); N. H. Christ, in *The Rice Meeting*, Proceedings of the Annual Meeting of the Division of Particles and Fields of the APS, Houston, Texas, 1990, edited by B. Bonner and H. E. Miettinen (World Scientific, Singapore, 1990), p. 780.
- [16] F. R. Brown, H. Chen, N. H. Christ, Z. Dong, W. Shaffer, L. I. Unger, and A. Vaccarino, *Phys. Lett. B* **251**, 181 (1990).
- [17] G. Bhanot and M. Creutz, *Phys. Rev. D* **24**, 3212 (1981).
- [18] A. D. Kennedy *et al.*, *Phys. Rev. Lett.* **54**, 87 (1985).
- [19] For $N_t = 2$: A. D. Kennedy, J. Kuti, S. Meyer, and B. J. Pendelton, *Phys. Rev. Lett.* **54**, 87 (1985). For $N_t = 4$: F. R. Brown *et al.*, *ibid.* **61**, 2058 (1989). For $N_t = 6, 8$, and 10: N. H. Christ and H. Q. Ding, *ibid.* **60**, 1367 (1988). For $N_t = 12$ and 14: N. H. Christ and A. E. Terrano, *ibid.* **56**, 111 (1986). For $N_t = 16$: N. H. Christ, in *Lattice '89* [8], p. 267.
- [20] For $N_t = 4$: F. R. Brown *et al.*, *Phys. Rev. Lett.* **65**, 2491 (1990); A. Vaccarino, Ph.D. thesis, Columbia University, 1991. For $N_t = 6$: C. Bernard *et al.*, *Phys. Rev. D* **45**, 3854 (1992). For $N_t = 8$: S. Gottlieb *et al.*, in *Lattice '91*, Proceedings of the International Symposium, Tsukuba, Japan, edited by M. Fukugita, Y. Iwasaki, M. Okawa, and A. Ukawa [*Nucl. Phys. B (Proc. Suppl.)* **26**, 308 (1992)].
- [21] For $N_t = 4$ and 6: A. Vaccarino, in *Lattice '89* [8], p. 441; F. R. Brown *et al.*, *Phys. Lett. B* **251**, 181 (1990); F. Butler, Ph.D. thesis, Columbia University, 1990; A. Vaccarino, Ph.D. thesis, Columbia University, 1991. For $N_t = 8$: R. Gavai *et al.*, *Phys. Lett. B* **232**, 491 (1989); **241**, 567 (1990).
- [22] G. 't Hooft, in *Recent Developments in Gauge Theories*, Proceedings of the Cargese Summer Institute, Cargese, France, 1979, edited by G. 't Hooft *et al.*, NATO Advanced Study Institute Series B: Physics Vol. 59 (Plenum, New York, 1980).
- [23] T. Banks and A. Zaks, *Nucl. Phys.* **B196**, 189 (1982).
- [24] Y. Iwasaki, in *Lattice '91* [20], p. 311; *Phys. Rev. Lett.* **69**, 21 (1992).